Ionization mechanism in the high power impulse magnetron sputtering (HiPIMS) discharge

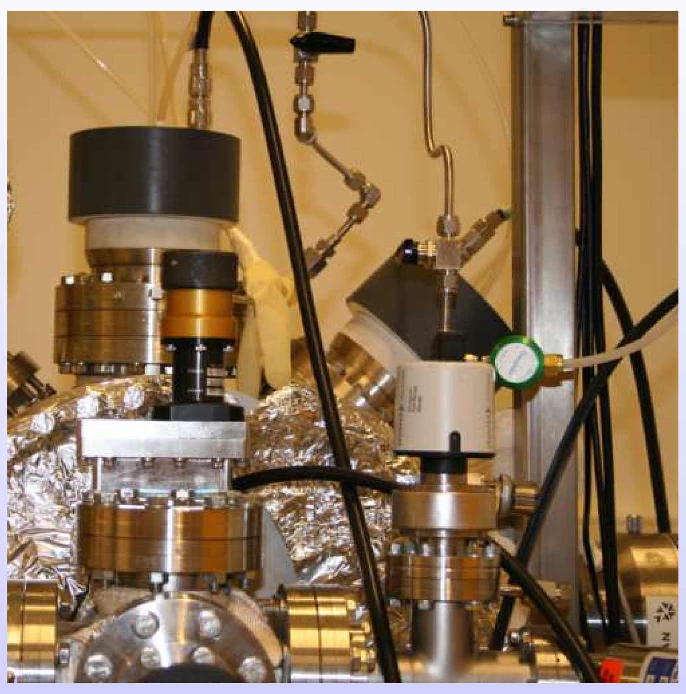

J. T. Gudmundsson

Science Institute, University of Iceland, Reykjavik, Iceland
Department of Electrical Engineering, University of Iceland, Reykjavik, Iceland
tumi@hi.is

Introduction

- In the high power impulse magnetron sputtering (HiPIMS) the discharge is created by applying a high power unipolar pulse of low duty cycle to the cathode target (Helmersson et al., 2005, 2006).
- The pulse length is typically 50 - 500 μs and the pulse frequency 1 – 1000 Hz
- The high power pulse has a peak cathode voltage in the range 500 – 2000 V which gives peak power densities in the range 1 – 3 kW/cm^2.
- A high fractional ionization has been demonstrated and values higher than 90 % have been reported (Bohlmark et al., 2005).
- The measured ionized flux fraction from Cu target was estimated roughly 70 % (Kouznetsov et al., 1999), from a $Ti_{0.5}Al_{0.5}$-target around 40 % (Macák et al., 2000), and from C and Al target 4.5 % and 9.5 %, respectively (DeKoven et al., 2003).
- The reported measured values are highly inconsistent.
- The ionization mechanism and the temporal behavior of the plasma parameters in a high power impulse magnetron sputtering (HiPIMS) discharge is investigated using a time dependent global (volume averaged) model.

The global (volume averaged) model

- The discharge is assumed to consist of electrons, Ar atoms in the ground state, metastable Ar atoms, Ar^+ ions, metal atoms, M, and metal ions, M^+.
- Electrons are assumed to have a Maxwellian energy distribution in the range 1 – 7 eV.
- The power balance equation, which equates the absorbed power $P_{\rm abs}$ to power losses due to elastic and inelastic collisions and losses due to charged particle flow to the discharge walls is given as

$$\frac{d}{dt}\left(\frac{3}{2}en_{\rm e}T_{\rm e}\right) = \frac{P_{\rm abs}}{V} - e\mathcal{E}_{\rm c}k_{\rm iz}n_{\rm Ar}n_{\rm e} - ek_{\rm wall,Ar^+}(\mathcal{E}_{\rm e}+\mathcal{E}_{\rm i})n_{\rm Ar^+} \quad (1)$$

where $\mathcal{E}_{\rm e}$ is the mean kinetic energy per electron lost and $\mathcal{E}_{\rm i}$ is the mean kinetic energy per ion lost, $m_{\rm i}$ is the argon ion mass, and $n_{\rm Ar^+}$ is the density of argon ions.

- The collisional energy loss per electron-ion pair created and is defined as

$$\mathcal{E}_{\rm c} = \mathcal{E}_{\rm iz} + \sum_{\rm i}\mathcal{E}_{{\rm ex},i}\frac{k_{{\rm ex},i}}{k_{\rm iz}} + \frac{k_{\rm el}}{k_{\rm iz}}\frac{3m_{\rm e}}{m_{\rm i}}T_{\rm e} \quad (2)$$

where $\mathcal{E}_{\rm iz}$ is the ionization energy, $\mathcal{E}_{{\rm ex},i}$ is the threshold energy and $k_{{\rm ex},i}$ is the rate coefficient for the i-th excitation process, respectively, $k_{\rm iz}$ is the ionization rate coefficient for single step ionization.

Reaction	k [m^3/s]
$e + Ar \longrightarrow Ar^+ + 2e$	$k_{\rm iz}$
$e + Ar \longrightarrow Ar^* + e$	$k_{\rm exc}$
$e + Ar^* \longrightarrow Ar^+ + 2e$	$k_{\rm exc,iz}$
$e + Ar^* \longrightarrow Ar + e$	$k_{\rm deexc} = 4.3\times10^{-16}T_{\rm e}^{0.74}$
$Ar^+ \longrightarrow Ar(wall)$	$k_{\rm wall,Ar+} = 2u_{\rm B}(h_{\rm L}R^2 + h_{\rm R}RL)/R^2L$
$Ar^* \longrightarrow Ar(wall)$	$D_{\rm Ar}\left[\left(\frac{\pi}{L}\right)^2 + \left(\frac{2.405}{R}\right)^2\right]$
$Ar^* \longrightarrow Ar + h\nu$	$k_{\rm rad}$
$e + Al \longrightarrow Al^+ + 2e$	$k_{\rm izm} = 1.23\times10^{-13}\exp(-7.23/T_{\rm e})$
$Al^+ \longrightarrow Al(wall)$	$k_{\rm wall,Al+} = 2u_{\rm B,m}(h_{\rm L}R^2 + h_{\rm R}RL)/R^2L$
$Al \longrightarrow Al(wall)$	$D_{\rm m}\left[\left(\frac{\pi}{L}\right)^2 + \left(\frac{2.405}{R}\right)^2\right]$
$Ar^* + Al \longrightarrow Al^+ + Ar + e$	$k_{\rm P} = 5.9\times10^{-16}$
$Ar^+ + Al \longrightarrow Al^+ + Ar$	$k_{\rm chex} = 1\times10^{-15}$

- The particle balance for the metal ions gives

$$\frac{dn_{\rm m+}}{dt} = k_{\rm miz}n_{\rm e}n_{\rm m} + k_{\rm P}n_{\rm Ar^*}n_{\rm m} + k_{\rm chexc}n_{\rm Ar^+}n_{\rm m} - k_{\rm wall,m+}n_{\rm m+} \quad (3)$$

where $n_{\rm m}$ is the neutral metal density, $n_{\rm m+}$ is the metal ion density, $n_{\rm Ar^*}$ is the density of metastable argon atoms, and $m_{\rm i,m}$ is the metal ion mass.

- The particle balance for metal atoms is

$$\frac{dn_{\rm m}}{dt} = \frac{h_{\rm L}r_{\rm T}^2}{R^2L}\left(\gamma_{\rm sput}u_{\rm B}n_{\rm Ar^+} + \gamma_{\rm selfsput}u_{\rm B,m}n_{\rm m+}\right)$$
$$-k_{\rm miz}n_{\rm e}n_{\rm m} - k_{\rm P}n_{\rm Ar^*}n_{\rm m} - k_{\rm chexc}n_{\rm Ar^+}n_{\rm m} - k_{\rm diff,m}n_{\rm m+} \quad (4)$$

where $\gamma_{\rm sput}$ is the yield of sputtered atoms per incident argon ion, $\gamma_{\rm selfsput}$ is the yield of sputtered atoms per incident metal ion, $r_{\rm T}$ is the target radius.

- The particle balance equation for generation and loss of metastable argon atoms is

$$\frac{dn_{\rm Ar^*}}{dt} = k_{\rm exc}n_{\rm e}n_{\rm Ar} - k_{\rm exc,iz}n_{\rm e}n_{\rm Ar^*} - k_{\rm deexc}n_{\rm e}n_{\rm Ar^*}$$
$$-k_{\rm loss,Ar^*}n_{\rm Ar^*} - k_{\rm P}n_{\rm Ar^*}n_{\rm m} \quad (5)$$

- The particle balance for argon ions is

$$\frac{dn_{\rm Ar^+}}{dt} = k_{\rm iz}n_{\rm e}n_{\rm Ar} + k_{\rm exc,iz}n_{\rm e}n_{\rm Ar^*} - k_{\rm chexc}n_{\rm m}n_{\rm Ar^+} - k_{\rm wall,Ar+}n_{\rm Ar^+} \quad (6)$$

- The temporal variation of the particle density and the electron temperature was obtained by solving the differential equations (1), (3), (4), (5) and (6) simultaneously and self-consistently. Once the density of Ar^+ and M^+ ions is found the quasi-neutrality condition gives the electron density $n_{\rm e} = n_{\rm Ar^+} + n_{\rm m+}$.

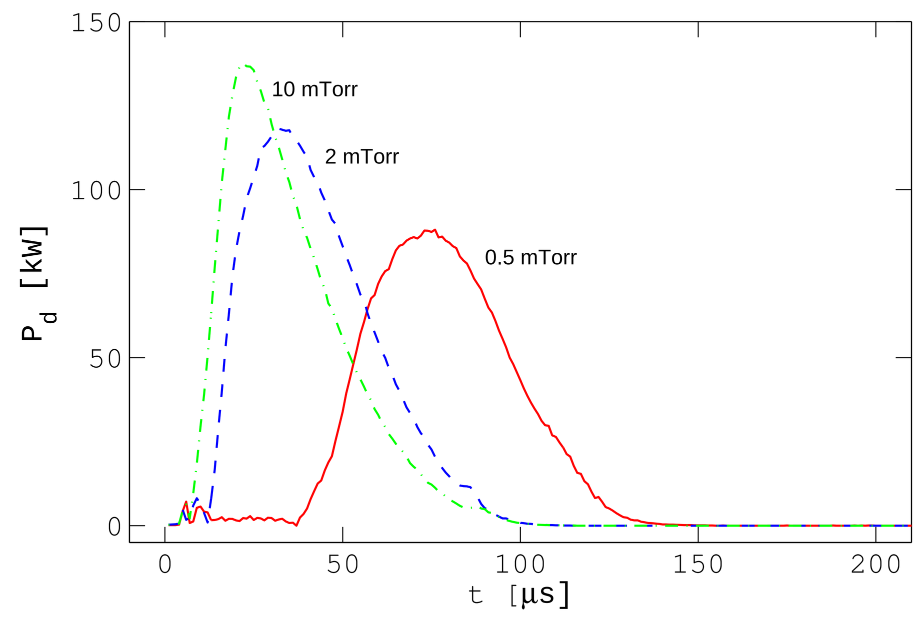

Figure 1: The measured power applied to the discharge versus time from the pulse initiation. The target was made of tantalum 7.5 cm in radius. After Gudmundsson et al. (2002).

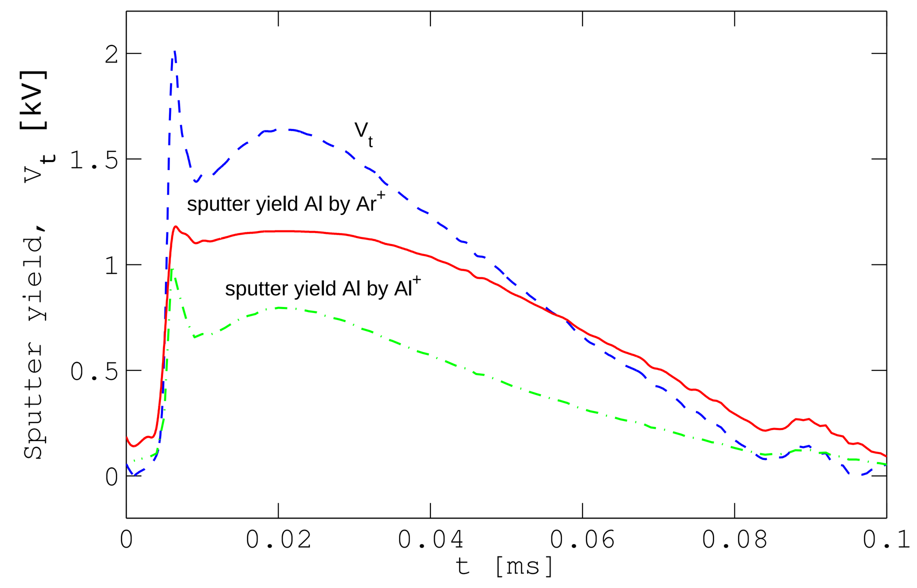

Figure 2: The sputter yield of Ar^+ on Al and Al^+ on Al versus time. The voltage applied to the discharge versus time from the pulse initiation determined experimentally at 10 mTorr. The target was made of tantalum 7.5 cm in radius.

Results and discussion

- To explore the ionization processes in a high power impulse magnetron sputtering discharge we assume a discharge chamber of radius R = 15 cm and length L = 15 cm with a target of radius 7.5 cm made of aluminum.
- We assume the power pulse to be the same as shown in figure 1 and the discharge pressure to be 10 mTorr (after Gudmundsson et al. (2002)).

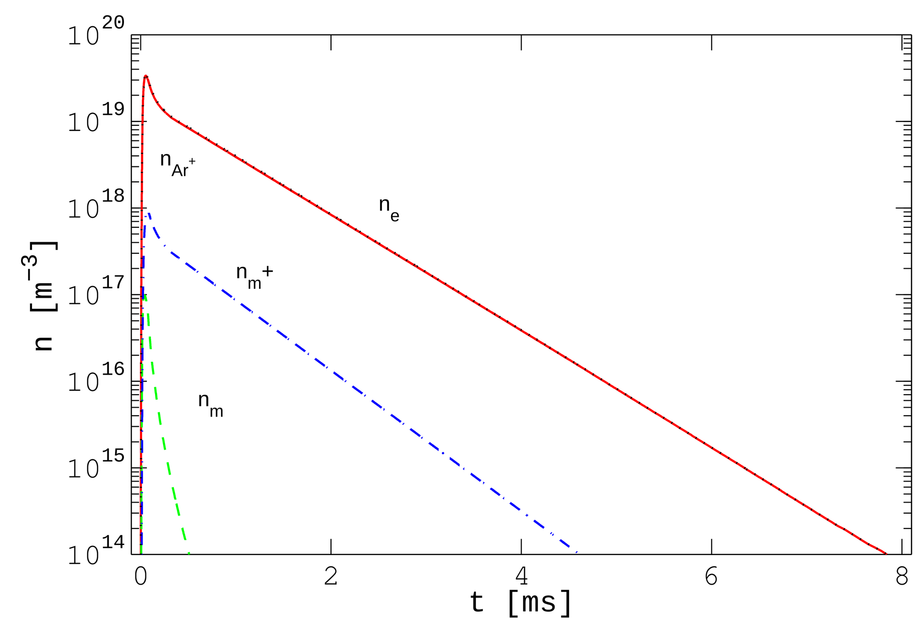

Figure 3: The calculated density of electrons, argon ions, aluminum ions and aluminum atoms versus time from the pulse initiation.

- The metal ion flux to the surface is $\Gamma_{\rm m+} \approx 0.61n_{\rm m+}u_{\rm B,m}$ and the flux of the neutral metal is $\Gamma_{\rm m} = \frac{1}{4}v_{\rm m}n_{\rm m}$.
- In discharges that are not in thermal equilibrium the electron temperature $T_{\rm e}$ is typically significantly larger than the neutral gas temperature $T_{\rm g}$. Thus, the fraction of ionized metal flux at the substrate $\Gamma_{\rm m+}/(\Gamma_{\rm m+}+\Gamma_{\rm m})$ is larger than the fraction of ionized metal in the plasma $n_{\rm m+}/(n_{\rm m+}+n_{\rm m})$.
- The integrated metal ion fraction is 0.98 and the integrated ionized flux fraction is 0.99 during the pulse.

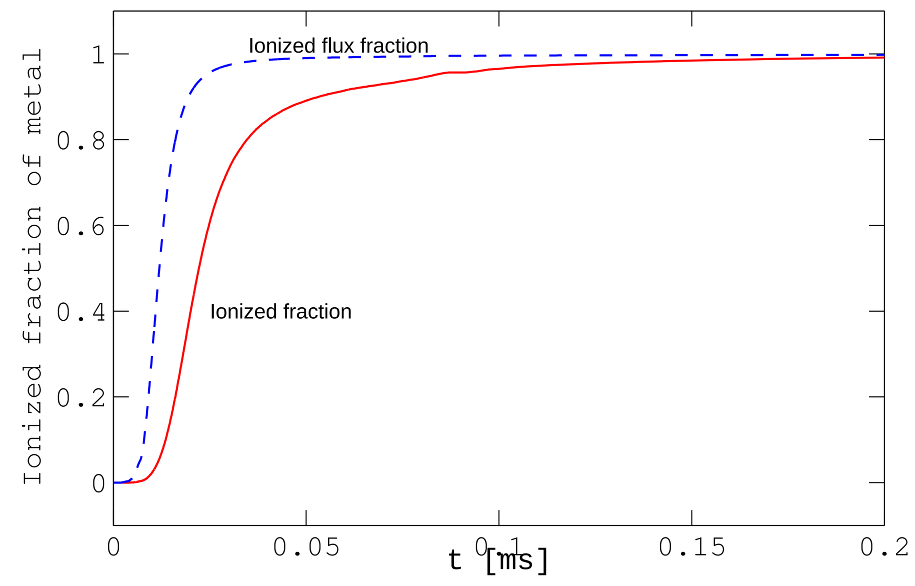

Figure 4: The ionized metal fraction and the ionized flux fraction versus time from the pulse initiation.

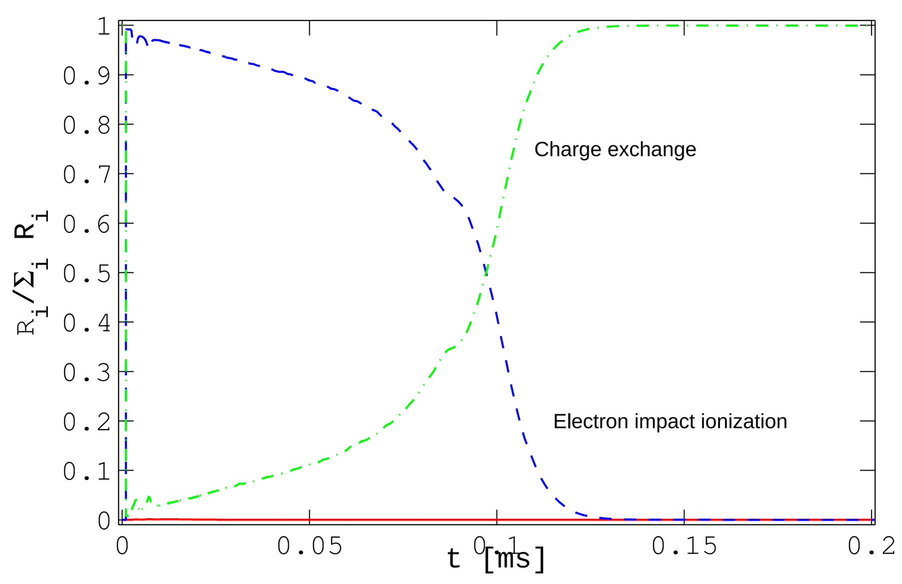

Figure 5: The relative reaction rate for the creation of the metal ion versus time from the pulse initiation.

Conclusions

- The metal ion fraction and the ionized flux fraction are very high, the sputtered metal is almost fully ionized.
- During the pulse on period electron impact ionization is the most effective process in creating metal ions while charge exchange becomes the dominant process in creating metal ions after the pulse is off.

Acknowledgments

This work was partially supported by the Icelandic Research Fund and the University of Iceland Research Fund.

References

U. Helmersson, M. Lattemann, J. Alami, J. Bohlmark, A. P. Ehiasarian, and J. T. Gudmundsson, in *48th Annual Technical Conference Proceedings* (Society of Vacuum Coaters, Denver, CO, USA, 2005), pp. 458 – 464.

U. Helmersson, M. Lattemann, J. Bohlmark, A. P. Ehiasarian, and J. T. Gudmundsson, Thin Solid Films **513**, 1 (2006).

J. Bohlmark, J. Alami, C. Christou, A. P. Ehiasarian, and U. Helmersson, Journal of Vacuum Science and Technology A **23**, 18 (2005).

V. Kouznetsov, K. Macák, J. M. Schneider, U. Helmersson, and I. Petrov, Surface and Coatings Technology **122**, 290 (1999).

K. Macák, V. Kouznetzov, J. M. Schneider, U. Helmersson, and I. Petrov, Journal of Vacuum Science and Technology A **18**, 1533 (2000).

B. M. DeKoven, P. R. Ward, R. E. Weiss, D. J. Christie, R. A. Scholl, W. D. Sproul, F. Tomasel, and A. Anders, in *46th Annual Technical Conferece Proceedings* (Society of Vacuum Coaters, San Francisco, CA, USA, 2003), pp. 158–165.

J. T. Gudmundsson, J. Alami, and U. Helmersson, Surface and Coatings Technology **161**, 249 (2002).